Wave localization in disordered and fractal systems

Vries, Pedro de; Raedt, Hans De; Lagendijk, Ad

Published in:
Computer Physics Communications

DOI:
10.1016/0010-4655(93)90046-F

Publication date:
1993

Computer Physics Communications 75 (1993) 298–310
North-Holland

Computer Physics Communications

Wave localization in disordered and fractal systems

Pedro de Vries [a,b], Hans De Raedt [a] and Ad Lagendijk [b,c]

[a] *Institute for Theoretical Physics, Nijenborgh 4, 9747 AG Groningen, The Netherlands*
[b] *Van der Waals–Zeeman Laboratorium, Valckenierstraat 65–67, 1018 XE Amsterdam, The Netherlands*
[c] *Foundation for Fundamental Research on Matter (FOM) – Institute for Atomic and Molecular Physics, Kruislaan 407, 1098 SJ Amsterdam, The Netherlands*

Received 17 August 1992

Numerical study of wave localization in systems with disorder and/or fractal characteristics is considered. Computational techniques employed entail solving the time-dependent Schrödinger equation for particular initial wave packets. Efficient and accurate numerical algorithms based on Trotter–Suzuki product formulas are presented. Propagation of light through a semi-infinite medium with disorder in the transverse directions is studied. It is shown that propagation of wave packets in one direction coexists with localization in the other two dimensions: We refer to this effect as transverse localization. Localization properties of quantum particles on fractal networks are investigated for two very well-known tight-binding models: The quantum percolation model and the fracton model. Spatial behavior of eigenstates is considered in connection with theoretical predictions of superlocalization. In disagreement with these predictions regular exponential behavior is found.

1. Introduction

1.1. Anderson localization

The presence of disorder may strongly affect both the nature of eigenstates and the motion of wave packets in otherwise translationally invariant media. For weak disorder e.g. wave packets scatter and motion becomes diffusive. It was first realized by Anderson [1] that, for strong disorder, interference effects of multiple scattered waves have a profound influence on the propagation of particles. Because of strong interference effects the particle becomes localized in some region of space. The probability of finding the particle outside this region decreases exponentially with distance. Eigenstates are now said to be localized. This phenomenon is called Anderson localization. The simplest model for localization is a tight-binding Hamiltonian describing noninteracting electrons in the presence of site disorder. This Anderson model for disorder has been the subject of extensive theoretical, experimental and numerical studies (for reviews see refs. [2,3]). These have led to the following insights. In $d \leq 2$ all eigenstates are exponentially localized for any strength of the disorder. In two dimensions, however, localization lengths become exponentially large as the disorder strength goes to zero. For three-dimensional systems each given energy requires a critical strength of disorder for eigenstates to become localized: There exists a mobility edge separating localized and extended states.

In the weak-disorder regime, also termed weak localization, perturbative approaches and diffusion theories are applicable. Studies along these lines have led to a number of important concepts in condensed matter physics: e.g. enhanced backscattering effects and long-range correlation phenomena (universal conductance fluctuations) in mesoscopic conductors [2,3]. In the limit of strong disorder transport quantities are zero and

Correspondence to: P. de Vries, Institute for Theoretical Physics, Nijenborgh 4, 9747 AG Groningen, The Netherlands.

all eigenstates are localized. Asymptotically, one then expects an exponential decay [4] for the envelope of localized eigenstates with an energy-dependent localization length.

The most popular numerical method used to study Anderson localization is the strip-and-bar technique combined with finite size scaling analysis [3,5–9]. The results of this technique confirm theoretical predictions for $d = 2$ and $d = 3$. The strip-and-bar technique is based on an exact iterative method for calculating localization lengths in $d = 1$. To get relevant results for higher dimensions one extrapolates (quasi-)one-dimensional results using scaling assumptions. A study employing direct numerical integration of the time-dependent Schrödinger equation (TDSE) on very large disordered lattices has shown [10] that for weak disorder this technique among others overestimates the localization length in $d \geq 2$.

It should be noted that Anderson localization is a wave interference phenomenon and not strictly a quantum effect. As such, it also applies to any other kind of wave phenomena. Examples are phonons and acoustic or electromagnetic (light) waves. In the low-energy limit electrons display s-wave scattering independent of the energy. Classical waves scatter very weakly in this limit, e.g. the cross-section for Rayleigh scattering of light is proportional E^4. Since localization is expected to set in for wavelengths λ of the order of the scattering mean free path l_{sc} (the so-called Ioffe–Regel criterion), the latter being inverse proportional to the cross-section, one sees that electrons generally localize easier than classical waves for low energies. In electronic systems electron–electron interaction effects play an important role. In the study of classical waves in disordered systems, wave interactions only appear when nonlinear effects are introduced. Weak localization of light has been studied extensively the past few years (for recent reviews see ref. [11]). Presently, the observation of strong localization of light still remains a challenging goal.

In this work we study localization properties in the strong disorder limit. This is done by solving the TDSE employing a numerical algorithm based on Trotter–Suzuki product formulas. The Trotter–Suzuki approximation and product formula algorithms are presented in section 2. In section 3 we present a new form of localization of light. We demonstrate by solving the TDSE that light in a medium with disorder in two directions propagates freely in one dimension and shows strong localization in the other two.

1.2. Localization and fractal geometry

In recent years, an enormous amount of theoretical and experimental work [12,13]* has been devoted to the description of vibrational properties of structures exhibiting fractal characteristics. Static and dynamic properties of fractal geometries can be described by a number of different noninteger exponents or dimensionalities. Many studies have concentrated on the dynamics of percolating networks. Percolating systems are Euclidian on length scales larger than the percolation correlation length ξ_p. For lengths below ξ_p the geometry is fractal and statistically self-similar. With ξ_p is associated an energy ω_c which separates two distinct regimes in the density of states (DOS) of vibrational excitations. For energies $\omega \ll \omega_c$ phonon-like behavior is expected: $\rho(\omega) \propto \omega^{d-1}$. For $\omega \gg \omega_c$ the DOS is no longer determined by the Euclidian dimension d but by the spectral dimensionality $\bar{\bar{d}}$[15,16]: $\rho(\omega) \propto \omega^{\bar{\bar{d}}-1}$. The excitations in the latter regime are termed fractons. The crossover in the DOS from phonon to fracton behavior has been observed in numerical calculations [17–20] and in experiments [14].

Alexander and Orbach have conjectured [15] that $\bar{\bar{d}}$ has a universal value of $\frac{4}{3}$ for percolation in $d \geq 2$. However, numerical calculations [21] of the conductivity exponent for two-dimensional percolation are not in agreement with the predicted value using $\bar{\bar{d}} = \frac{4}{3}$. In addition, it has been shown that the spectral dimension is not universal. Experiments [14] and numerical simulations [22] show that $\bar{\bar{d}}$ depends on the microstructure of the fractal network. For increasing connectivity

* The majority of experimental work on percolation systems in relation with fractal dynamics has been performed on silica aerogels. For a short review of these studies involving neutron, Brillioun and Raman spectroscopic techniques see ref. [14].

(e.g. no dangling ends and/or interactions between particles beyond nearest neighbors) values for the spectral dimension increase. For the backbone of percolation clusters one finds [13] $\bar{\bar{d}} < \frac{4}{3}$. Moreover, simulations [23] for tensorial elastic vibrations indicate that $\bar{\bar{d}} \approx 0.8$. Although the Alexander–Orbach conjecture is probably not exact for all d, it nevertheless turns out to be a very good approximation for scalar vibrations as numerical simulations have shown [17–20].

Until recently, not much was known about the spatial behavior of fractons. The lack of translational invariance and the presence of geometric disorder in fractal media suggest that excitations might be spatially localized [3]. In the Euclidian regime of percolation networks vibrational excitations will follow the usual Anderson localization behavior. For fractal geometries it has been suggested [16] that the relevant dimensionality concerning localization is the spectral dimension $\bar{\bar{d}}$. Since for percolation $\bar{\bar{d}} \simeq \frac{4}{3}$, which is smaller than two, all excitations in the fractal regime (fractons) are also expected to be localized. The scaling model for fractons [12,24] predicts that (scalar) fractons are characterized by *one* single length scale. The localization length $l(\omega)$ and the wavelength $\lambda(\omega)$ are assumed to be proportional to one another and to be of the same order, so that the former should display the same scaling behavior as the latter [12,24]:

$$l(\omega) \propto \omega^{-\bar{\bar{d}}/D}. \tag{1.1}$$

This behavior is contrary to Anderson localization for electrons, in which localization lengths decrease with decreasing energy.

A very important question is whether fractal geometry can alter the usual exponential behavior associated with Anderson localization. For localized states in fractals the following asymptotic spatial behavior for the vibrational amplitude (or Schrödinger wave function with energy $E = \omega^2$) has been proposed [24–26]

$$|\Psi(r;\omega)| \propto l(\omega)^{-D/2} \exp\left\{-\tfrac{1}{2}(r/l(\omega))^{d_\phi}\right\}, \tag{1.2}$$

where $l(\omega)$ is the energy-dependent localization length and $D(\leq d)$ is the fractal dimension. One should bear in mind that the wave functions (1.2) are defined only on the fractal structure, while r denotes a Euclidean distance measured in the embedding space. The superlocalization exponent $d_\phi (> 1)$ is expected to be related to some relevant geometry of paths on the fractal [24–26]. Different theoretical values have been proposed for d_ϕ. Lévy and Souillard predict [25] $d_\phi = \frac{1}{2} d_w > 1$, where d_w describes the anomalous diffusion of a classical random walker. Rigorous arguments for the quantum percolation model, see below, connect [26] d_ϕ to the (static) chemical-length exponent ζ_c. Values of the localization exponent for *one* arbitrary wavefunction should typically lie in the interval $1 \leq d_\phi \leq \zeta_c$. Averaging over *all* solutions would then result [26] in regular exponential behavior $d_\phi = 1$. It has also been proposed [24] that $d_\phi = \tilde{\zeta}$, where $\tilde{\zeta} = d_w - D$ describes the scaling with distance of the resistivity between two points [13]. The resistivity exponent is always smaller than the chemical-length exponent.

In section 4 numerical calculations of the dynamics of a *quantum* particle on two-dimensional percolation networks are presented and discussed. Two tight-binding models defined on these networks are investigated: the fracton model, equivalent to the classical fractons above, and the quantum percolation model. The characterization of the spatial behavior of eigenstates will be of particular interest. Scaling predictions for the energy dependence of localization lengths, see (1.1), are checked. The asymptotic spatial behavior is investigated.

2. Computational techniques

2.1. Time-dependent Schrödinger equation

Dynamical properties of quantum models can be studied fruitfully by solving the time-dependent Schrödinger equation (TDSE) numerically and extracting the desired physical information from the time development of suitably chosen wave packets. Given an initial wave function $\Psi(t = 0)$ the formal solution of the TDSE,

$$\frac{\mathrm{d}}{\mathrm{d}t}\Psi(t) = -\mathrm{i}H\Psi(t), \tag{2.1}$$

where H is the Hamiltonian of the model under consideration, is written as

$$\Psi(t) = e^{-itH}\Psi(t=0). \tag{2.2}$$

All dynamical information is contained in the solution $\Psi(t)$.

The fundamental problem here is the computation of the unitary evolution operator $\exp(-itH)$ for which in general an approximation is needed. Obviously, only Hamiltonians of small systems can be diagonalized numerically giving all relevant information. This is in particular a serious drawback for localization problems where system sizes should be larger than some typical localization length. Clearly, for (very) large systems another strategy is required. Depending on the specific physical property to be studied, several approaches may be possible. For instance, the spectrum of a Hamiltonian may be calculated using either recursion (Lanczos) techniques or the equation-of-motion method of Alben et al. [27], in which the TDSE is solved numerically and particular time-dependent solutions are analyzed. It has been demonstrated that both methods are comparable in efficiency provided a high-order algorithm is used in the latter case [28]. For the low-order leap-frog algorithm it was shown how to correct for various artifacts, so that large time steps are in fact possible [29]. In connection with applications to models with disorder it has also been pointed out that the interpretation of propagating wave packets is much clearer than that of wave functions obtained from recursion methods [28,30].

Having chosen a suitable representation or "lattice" for the Hamiltonian H the next step in an integration procedure for solving the TDSE is to make an approximation for the evolution operator $\exp(-i\tau H)$ for some time step τ. Repeated application of this approximate evolution operator then yields the solution $\Psi(t)$. Usually, either a polynomial approximation is made or the Crank–Nicholson method is used. The former approach leads to a non-unitary time-step operator, which does not conserve the norm of the wave function. In this case the numerical method may in principle create or annihilate "particles" during the integration procedure. This approach also requires the time step τ to be sufficiently small for the numerical method to remain stable, i.e. to assure that errors due to the approximation and to finite computer precision will not grow exponentially. Construction of unitary approximants to $\exp(-i\tau H)$ give unconditionally stable numerical techniques, because unitarity implies conservation of the norm of wave functions. The Crank–Nicholson method leads to a unitary approximant. This method, however, is an implicit one since at each time-step a set of linear equations has to solved or, equivalently, a matrix has to be inverted. Due to its implicit character this approach is not very efficient, except for one-dimensional problems.

The approach adopted here is to make use of generalizations of Trotter's product formula [31] which were first proposed by Suzuki [32,33]. During the last decade these product-formula approximants to exponential operators have been instrumental in the rapid and successful development of quantum Monte Carlo methods for quantum-statistical lattice models (for a review see ref. [34]). A recent development has been the construction of accurate and efficient algorithms employing the Trotter–Suzuki approximation scheme to solve the TDSE [35]. Within this approximation it is possible to devise time-step evolution operators defined as some ordered product of unitary operators. Therefore, by construction the approximant to $\exp(-i\tau H)$ is unitary and algorithms based on these approximants are unconditionally stable. It must be noted that product-formula-type techniques have also been developed independently for applications in high-resolution electron microscopy [36] and problems concerning propagation of light in optical fibers. [37]

The method of analysis of solutions $\Psi(t)$ depends on the physical quantity of interest and usually is rather straightforward [27,35,38]. Closely related to this is the choice of the initial wave function at $t = 0$.

2.2. *Product-formula algorithms*

The basic idea underlying applications of the Trotter–Suzuki approximation is the fact that a

particular Hamiltonian H can generally be decomposed into a number of operators $\{H_k\}$, where each operator H_k can independently be diagonalized analytically. Subsequently, exponential time-step operators $\exp(-i\tau H_k)$ are computed straightforwardly. Having chosen a particular decomposition of the Hamiltonian, $H = \sum_{k=1}^{K} H_k$, several unitary approximants to the evolution operator $\exp(-i\tau H)$ as a product of operators $\exp(-i\tau H_k)$ can be constructed.

An important characteristic of any algorithm is its accuracy, which is determined here by the "local" error involved with the specific approximant to the time-step operator

$$\exp(-i\tau H) = U_n(\tau) + \mathcal{O}(\tau^{n+1}). \tag{2.3}$$

The index n indicates to which order in the time step τ the approximant $U_n(\tau)$ exactly represents $\exp(-i\tau H)$. The "global" error on the wave function at time $t = m\tau$ is given by the root-mean-square (RMS) error $|\exp(-itH)\,\Psi(0) - (U_n(\tau))^m \Psi(0)|$. Assuming all local errors to add up independently the RMS error can be shown to be bounded from above by $r_{(n)} t \tau^n$, where for the approximants presented below $r_{(n)}$ is the norm of some commutator expression involving the operators $\{H_k\}$ [35,39,40].

The simplest approximant, having a local error $\mathcal{O}(\tau^2)$, is the first-order approximant

$$U_1(\tau) = e^{-i\tau H_1} e^{-i\tau H_2} \cdots e^{-i\tau H_{K-1}} e^{-i\tau H_K}. \tag{2.4}$$

Second-order algorithms follow by using symmetrized expressions [35,41]

$$U_2(\tau) = e^{-i\tau/2H_1} \cdots e^{-i\tau/2H_{K-1}} e^{-i\tau H_K} \times e^{-i\tau/2H_{K-1}} \cdots e^{-i\tau/2H_1}. \tag{2.5}$$

Since the study of some physical properties in this work require the solution of the TDSE for very large times we have used higher-order algorithms. With $H = H_1 + H_2$ the fourth-order approximant [35,41]

$$U_4(\tau) = e^{-i\tau/2H_1} e^{-i\tau/2H_2} e^{i\tau^3[H_1+2H_2,[H_1,H_2]]/24} \times e^{-i\tau/2H_2} e^{-i\tau/2H_1}, \tag{2.6}$$

can be derived. Because of the τ^3 dependence the second exponential operator can be factorized further using a first-order approximant. In most applications to date eq. (2.6) has been used iteratively. (This is also the case for second-order approximants.) For example, in a fourth-order algorithm a Hamiltonian consisting of kinetic energy T and potential energy V is first decomposed into $H_1 = T$ and $H_2 = V$ and, subsequently, the kinetic energy T is decomposed further using an odd and even sublattice breakup [35]. In the present work eq. (2.6) has been used throughout; no use has been made of split-step fast Fourier transform techniques.

Very recently, Suzuki developed [42] a new approach for obtaining high-order product formula approximants to $\exp(H_1 + \cdots + H_K)$. A convenient fourth-order approximant reads [42]

$$\tilde{U}_4(\tau) = (U_2(p\tau))^2 U_2((1-4p)\tau)(U_2(p\tau))^2, \tag{2.7}$$

where $U_2(\cdot)$ is the second-order approximant (2.5), and $p = 1/(4 - \sqrt[3]{4})$. Note that no commutators appear in this new approximant, so that its implementation on a computer is easier than that for eq. (2.6).

All of the above approximants are unitary by construction and yield an unconditionally stable algorithm conserving the norm of the wave function. Naturally, the decomposition of the Hamiltonian must be such that each $\exp(-i\tau H_k)$ can be diagonalized analytically. In this approach the computational effort for sparse matrices H scales linearly with system size N for any dimension. Furthermore, the action of each unitary operator on a wave function can be chosen such that pairs of lattice points can be treated independently and simultaneously [35]. Because of this parallelism product-formula algorithms are easily implementable on vector processors. It must also be noted that the Hamiltonian does not commute with the approximants $U_n(\tau)$, so that in principle the energy is not conserved. In practice, however, the RMS errors on the wave function are much larger than those on expectation values involving H. For very long simulations the accuracy in the energy is still typically at least three digits.

3. Transverse localization of light

A new form of localization of light is introduced in which the wave is propagating in one direction but confined in the other two. We call this effect "transverse localization". If the index of refraction is a random function of (x, y) but is constant in the positive z direction, it is shown that a wave coming in from the negative z direction propagates in the positive z direction and expands until the beam diameter becomes of the order of the transverse localization length. From then on, the beam propagates without further expansion or, in other words, behaves as if it is going through a "random fiber".

It is shown first that the problem can be mapped onto the time-dependent two-dimensional Schrödinger equation with the z coordinate having the role of time. Consider a medium of which the index of refraction is homogeneous in one direction. Propagation of waves through this medium is governed by the scalar Helmholtz equation (for simplicity the scalar form of the Maxwell equation is used) [43]

$$\nabla^2\phi + k^2 n^2(x, y)\phi = 0, \tag{3.1}$$

where $k = 2\pi/\lambda$, $n(x, y)$ is the index of refraction at the point (x, y, z). In general, n depends on the angular frequency $\omega = 2\pi c/\lambda$. Since only monochromatic light is considered, the ω dependence of n has been omitted. From an experimental point of view, it is essential to see how an incoming wave behaves. For this one needs to consider a semi-infinite system, instead of an infinite system extending from $z = -\infty$ to $z = +\infty$. In the latter case, the z dependence of the wave field trivially factors out. Writing for the former $\phi(x, y, z) = \psi(x, y, z)\exp(-ikn_0 z)$ and employing the argument that if

$$\left|\frac{\partial^2\psi}{\partial z^2}\right| \ll 2kn_0\left|\frac{\partial\psi}{\partial z}\right|, \tag{3.2}$$

eq. (3.1) reduces to the paraxial form of the wave equation

$$2ikn_0\frac{\partial\Psi}{\partial z} = H\Psi, \tag{3.3}$$

where the symbol Ψ has been introduced to distinguish the solution Ψ of the parabolic approximation (3.3) from the solution $\phi(\psi)$ of the elliptic problem (3.1), H is defined by

$$H \equiv \partial^2/\partial x^2 + \partial^2/\partial y^2 + k^2\left[n^2(x, y) - n_0^2\right]. \tag{3.4}$$

Above, an effective index of refraction $n_0^2 \equiv \int n^2(x, y)\,dx\,dy/(\text{area})$ has been introduced. H resembles the Hamiltonian for a quantum particle moving in a random potential with zero mean. Hence, it is expected that interference will cause the wave field to be exponentially localized in the (x, y) plane. If localization occurs, one expects that the incoming wave will not spread in the transverse direction beyond the localization length. Otherwise, the beam will continue to expand. Of course, upon integrating the TDSE (3.3) the solution will have to satisfy requirement (3.2). We emphasize that (3.1) and (3.3) only differ in the way the propagation of light in the $z > 0$ direction is described; the properties of the field in the (x, y) plane are the same for both equations [44].

The simulated model consists of a bar of dimensions $L \times L \times L_z$ in which " fibers" of length d, width d, and height L_z are defined. A randomly chosen fraction p of these "fibers" has a real refractive index n_2; the remainder of the volume has a real index of refraction $n_1 (< n_2)$. At the (x, y) plane at $z = 0$ a Gaussian beam of monochromatic coherent light enters the sample perpendicularly. The center of the beam coincides with the center of the $z = 0$ plane. The area on the entrance plane covered by the incident beam of light is assumed to be much less than the area L^2 of the entrance plane itself. The Gaussian width b of the beam is chosen much larger than the wavelength of the light to avoid difficulties in describing the diffraction properties of the beam. All distances are in units of the wavelength λ. The mesh size δ of the two-dimensional lattice used in the simulations is chosen such that variations of Ψ as a function of x or y are smooth on a scale of the mesh size. Computations were carried out with $0.25\ \lambda \le \delta \le \lambda$, up to 76800 "time" steps using lattices of 401×401 sites. Parameters used were $b = 10\lambda$, $d = 4\lambda$, which is

not unrealistic, $n_1 = 1$ and $n_2 = 1.25(1.5)$, the latter being within the range of refractive indices of existing materials, $z \leq 24\,000\lambda$ (6000λ), and $p = \frac{1}{2}$.

Various tests have been performed. For example, if there is only *one* "fiber" with $n_2 > n_1$ placed at the center of a large sample $(d \ll L)$, waveguide behavior should result. This behavior is also found in our simulations. The light is localized but certainly not as a consequence of randomness. Consider next the situation with "fibers" with refractive index n_2 placed randomly in accordance with the filling factor p (p is below the percolation threshold $p_c = 0.5927$). For $\lambda \ll d$ there is little probability of having amplitude traversing through one of the "potential" barriers. In this case the system resembles a collection of fibers varying in size and shape. Within each of these waveguides the wave field is, for all practical purposes, localized in the same sense as above. Evanescent waves are negligible in this case. The most interesting situation arises when $\lambda \approx d$ and $p = \frac{1}{2}$. Then the wave field is able to "tunnel" through the potential barriers where it can interfere with light that has arrived there by taking different routes. In all our simulations the right-hand side of (3.2) was found to be a factor of 10 larger than the left-hand side, suggesting that the inequality is reasonably well satisfied.

In fig. 1 representative results are presented for the case $n_2 = 1.5$. The solid line, being proportional to the central second moment of $|\Psi|^2$ [35], $\xi(z) \propto (\langle \Psi(z) | r^2 | \psi(z) \rangle - \langle \Psi(z) | r | \Psi(z) \rangle^2)^{1/2}$, where r is the vector to a point in the (x, y) plane, is a measure for the width of the amplitude of the wave field. From fig. 1 one sees that initially the wave field expands, essentially as a free field for which $\xi(z) \propto z$, but then it asymptotically approaches a constant value. The remaining fluctuations reflect the intrinsic interference phenomena ("speckles"). For sufficiently large z, $\xi(z)$ fluctuates around a finite value which is directly proportional to the localization length. To test whether the wave field decays exponentially for large z, $\xi(z)$ has also been calculated with the fourth moment, and from the dashed line in fig. 1 it can be concluded that the agreement is good.

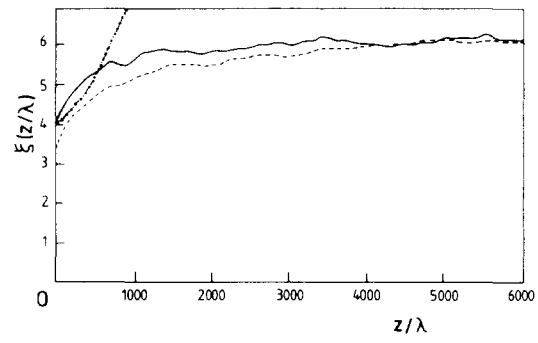

Fig. 1. Width of the wave field $\xi(z)$ (in units of λ) as a function of the length of the sample z. Solid line: estimate based on the second moment of $|\Psi|^2$ (localized behavior). Dashed line: estimate based on the fourth moment of $|\Psi|^2$. Dotted line: $\xi(z)$ for a uniform medium $p = 0$ (ballistic behavior).

In summary, direct numerical evidence has been given that a collection of randomly placed scattering "cylinders" or "fibers" will exhibit two-dimensional strong localization of light.

4. Fractal dynamics

4.1. Tight-binding models

Next, site-percolating networks on $L \times L$ square lattices are considered. Attention is confined to the "infinite" percolating cluster at the critical percolation concentration $p_c = 0.593$. This cluster exhibits fractal characteristics on all length scales with a fractal dimension $D = 91/48$. Two tight-binding Hamiltonians defined on these percolating lattices are studied:

$$H_1 = -V \sum_{\langle i,j \rangle} t_{ij} \left(c_i^\dagger c_j + c_j^\dagger c_i \right), \tag{4.1}$$

$$H_2 = H_1 + V \sum_{i=1}^{N} z_i c_i^\dagger c_i, \tag{4.2}$$

where in H_1 the summation is over nearest neighbors, $c_i^\dagger (c_i)$ creates (annihilates) a particle at site i, V is the interaction constant (set to unity in the following), $t_{ij} = 0$ or 1 depending on the absence or presence of a nearest neighbor and z_i is the coordination number of site i. The first

Hamiltonian (4.1) corresponds to the quantum percolation problem describing a binary alloy and has been studied extensively, [45,46]. It can be regarded as an Anderson Hamiltonian in which the site energies are chosen randomly to be 0 with probability p and ∞ with probability $1-p$. Therefore, behavior similar to the Anderson model could be expected. At the classical threshold p_c all quantum states should be localized with a finite localization length depending weakly on energy.

The second Hamiltonian (4.2) has an additional random diagonal part in which the site energies are proportional to the local coordination number. The numbers $\{z_i\}$ can be mapped one-to-one onto the numbers $\{t_{ij}\}$; both sets of numbers represent the configuration in question uniquely. So, the additional randomness introduced in the diagonal part of (4.2) is highly correlated with the off-diagonal term. For this reason Hamiltonian (4.2) cannot be regarded as a regular Anderson model and different behavior from (4.1) should be expected. This model can be mapped exactly onto a master equation describing a classical random walker on percolating networks or onto the vibrational problem of such structures; see the fracton model described in section 1.2 [15].

For both models we have computed [47] the density of states. Results were in agreement with theory and previous numerical calculations. For the fracton model, in particular, the lower band edge exhibited the power-law behavior $\rho(E) \propto E^{(\bar{\bar{d}}-2)/2}$ $(E \downarrow 0)$, where, in accordance with the conjecture $\bar{\bar{d}} = \frac{4}{3}$, it was found that $\bar{\bar{d}} = 1.34 \pm 0.02$ [47].

4.2. Localization properties

Whether states are localized or not can be investigated by considering the propagation of wave packets. Constructing wave packets of small sizes at $t = 0$ and measuring central second moments $\langle r^2(t)\rangle$ of the time-dependent probability distributions $|\Psi(r, t)|^2$ gives an insight into the nature of the eigenstates. In fig. 2 results are presented for the case that the particle initially is put on one site near the center of the lattice.

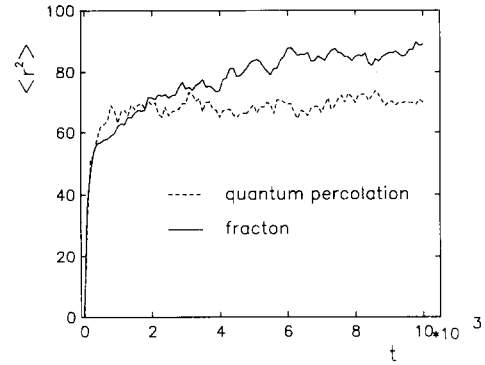

Fig. 2. Averaged central second moment as a function of time for particles put on one site at $t = 0$ and propagating on percolating square lattices. Levelling off indicates localization of particles.

Data shown are averages over fifteen runs on 200×200 square lattices with mean size $N = 12\,000$. The solid and dashed curves correspond to the fracton and quantum percolation model, respectively. The wave packets initially expand very rapidly. Next, for the fracton model, the propagation is diffusion-like ($\langle r^2(t)\rangle \propto t$) during a certain time interval. Eventually, the second moment tends to become saturated at a finite value. For quantum percolation the wave packet becomes localized almost immediately after its initial rapid expansion. The second moment fluctuates around a finite value. Assuming monotonic exponential behavior for the localized eigenstates, the central second moment reads $\langle r^2\rangle = 6l^2$. For quantum percolation one thus obtains for the wave packet $l \simeq 3.5$, a value well below system sizes used. For this model a smooth energy dependence of the localization length is expected. For fractons the localization length $l(E)$ diverges at the lower band edge $(0 < E < 1)$ as $E^{-\bar{\bar{d}}/2D}$, see (1.1). The diffusive behavior and the seemingly slow convergence to a finite value of the second moment may then be attributed to the low-energy eigenstates participating in the wave packets. At time $t = 10\,000$, however, the wave packet clearly can be considered to be localized.

Wave packets can also be constructed by diagonalizing a small $M \times M$ $(M \ll N)$ subsystem. In this way the spectral content of wave packets can more or less be adjusted. The energy uncertainty $\sigma_E \equiv \sqrt{\langle H^2\rangle - \langle H\rangle^2}$ is a measure for the spec-

tral width. For these wave packets similar characteristics were observed [47].

The energy dependence of localization lengths is investigated employing a technique in which averaged inverse participation numbers (IPN) are computed using all the relevant eigenstates of the lattice. This technique involving solutions of the TDSE has been developed by Weaire and Williams [38]. The inverse participation number of a normalized eigenstate ϕ is defined by

$$\mathscr{P}^{-1}(E) = \sum_i |\phi(\boldsymbol{r}_i)|^4. \tag{4.3}$$

For extended states $\mathscr{P}$ scales with the number of lattice sites; for localized states (with arbitrary d_ϕ) $\mathscr{P} \sim l(E)^D$. One should note that IPN depend on the precise shape of the wave function. Amplitude fluctuations may modify absolute values of the IPN. Employing scaling result (1.1) in the case of fractons, $\mathscr{P}(E)$ should behave like $E^{-\bar{\bar{d}}/2}$. Verifying this scaling result thus amounts to computing the fracton exponent $\bar{\bar{d}}$ from IPN.

In fig. 3 participation numbers $\mathscr{P}$ as a function of energy are shown for the two models. The bars on the energy are a measure of the energy interval determining $\mathscr{P}$. Finite-size effects are unimportant, since participation numbers are much smaller than the lattice sizes (100×100 and 200×200) used. As expected, for quantum percolation a smooth behavior as a function of energy is found. For this model results are an even function of energy (the band center is at $E = 0$). All states are localized with a finite localization length of the order $l \approx 5$. The density of states has two inner tails or gaps at the center of the band explaining why l decreases as $|E| \to 0$.

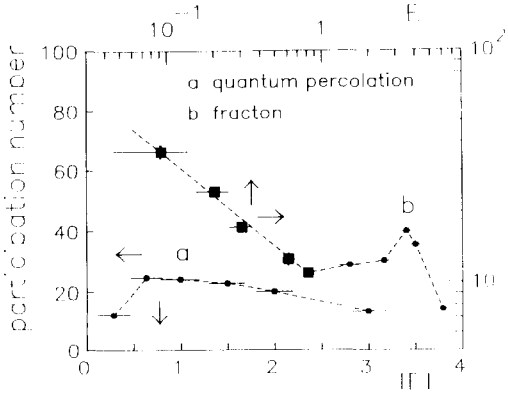

Fig. 3. Participation numbers as a function of energy. •: averaged data from six runs on 100×100 lattices with mean size $N = 3400$. ■: single run on a 200×200 lattice with size $N = 12064$. Error bars not shown have the size of the symbols. Lines are guides to the eyes. Participation numbers are a measure for the localization length of eigenstates.

The fracton model exhibits a power-law behavior at the lower band edge ($E < 1$) in accordance with theory [15,16]. For energies $E > 1$ localization lengths are of the order of the lattice unit. Extending the approach of Weaire and Williams, an improved analysis for very low energies of IPN, and a higher-order generalization, gave $\bar{\bar{d}} = 1.23 \pm 0.12$ and $\bar{\bar{d}} = 1.38 \pm 0.12$, respectively [48]. These values are in agreement with the conjectured value $\bar{\bar{d}} = \frac{4}{3}$. The conclusion is that at the lower band edge localization lengths of fractons do indeed scale as $E^{-\bar{\bar{d}}/2D}$. Recent calculations [49,50] have also confirmed this scaling behavior.

4.3. Asymptotic spatial behavior of waves

To test the various predictions concerning the superlocalization exponent (see eq. (1.2)) the asymptotic spatial decay of excitations is investigated for the two models. For percolation clusters in two dimensions, predicted values for the exponent d_ϕ are, respectively, $d_\phi = \frac{1}{2}d_w = 1.43$, $d_\phi = \zeta_c = 1.13$, and $d_\phi = \tilde{\zeta} = 0.975$ [13,21,25,26,51].

To simplify the analysis, one-dimensionally integrated probability distributions $I(x) = \sum_y |\Psi(x, y)|^2$ and $I(y) = \sum_x |\Psi(x, y)|^2$ of wave packets Ψ are studied [52]. From the spatial characteristics of wave packets the behavior of eigenstates is inferred. The propagating wave packets can be expressed in terms of eigenstates $\{\phi_n\}$ and energy eigenvalues $\{E_n\}$ as $\Psi(t) = \sum_n \alpha_n \exp(-iE_n t)\phi_n$, where $\{\alpha_n\}$ are expansion coefficients. By time averaging the probability distributions $|\Psi(t)|^2$ one finds that the resulting spatial behavior is determined by the "incoherent" sum $\sum_n \alpha_n^2 \phi_n^2$. In the calculation of the Green's function a particle is put on the center of the lattice at $t = 0$. In this case, the wave packets contains contributions form the whole spectrum. For a spectrum with comparable finite localiza-

tion lengths, as is the case for the quantum percolation model, see previous section, the asymptotic decay of wave packets is similar to that of its constituents and is determined by some typical l. For the fracton model this argument only strictly holds for packets with components that do not lie at $E \approx 0$. The latter can be achieved by diagonalizing a small $M \times M$ ($M \ll L$) subsystem. In this way the energy uncertainty, as measured by $\sigma_E^2 = \langle H^2 \rangle - \langle H \rangle^2$, can be reduced greatly, indicating that participating eigenstates lie substantially in a small energy interval. In the previous subsection (also see fig. 2) the propagation of wave packets has been discussed.

In fig. 4 the time-averaged probability distribution $\bar{I} \equiv \frac{1}{2}(\bar{I}(x) + \bar{I}(y))$ is presented for particles put initially on one site for the quantum percolation model. The result represents averages over twenty runs performed on 200×200 percolating lattices at p_c with mean size $N = 12000$. Wave packets were evolved in time up to $t = 10000$. The distributions exhibit exponential-like behavior. For the fracton model exponential-like tails were also found for the averaged Green's function distribution.

In fig. 5 probability distributions $I(x)$ and $I(y)$ of a wave packet with $\langle H \rangle = 0.19$ and $\sigma_E = 0.05$ are presented for the fracton model. This state was obtained by diagonalizing a 19×19 subsystem. Exponential-like tails can be seen. A pronounced decrease in probability is clearly observed. Similar results have been obtained for wave packets having different mean energies $\langle H \rangle$

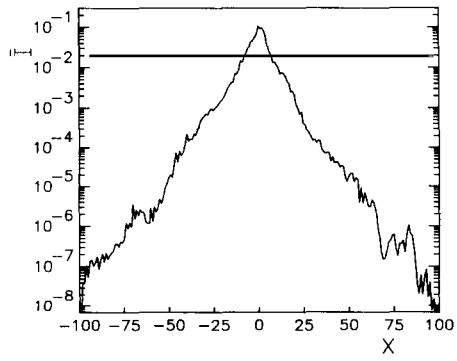

Fig. 4. Time-averaged probability distribution of the Green's function for the quantum percolation model. Average over twenty runs. Exponential-like tails are observed.

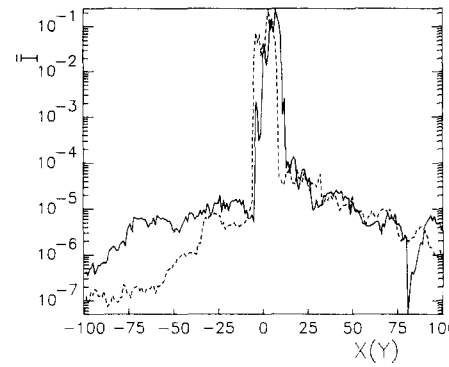

Fig. 5. Time-averaged one-dimensionally integrated probability distributions $\bar{I}(x)$ and $\bar{I}(y)$ for a wave packet with $\langle H \rangle = 0.19$ and $\sigma_E = 0.05$. Initial state was obtained by diagonalizing a 19×19 subsystem for the fracton model. Dashed curve: $\bar{I}(y)$. Two basic features are clearly shown: a short-ranged bulk-like structure and asymptotic tails.

and energy uncertainties σ_E employing both the fracton model and the quantum percolation model.

For the two models probability distributions generally show two basic structures. The majority of the probability is localized in "microclusters" which are attached to the macroscopic cluster by a few bonds. This feature has also been demonstrated by recent calculations [49] on the fracton model. The second basic structure is the asymptotic behavior displaying exponential-like tails. This behavior is similar to a particle localized in a potential well having random size and shape. The size of the random potential well essentially determines the localization length as calculated in the previous subsection with IPN. Outside the well the probability distribution asymptotically exhibits exponential decay. The boundaries of such a "microcluster" may be reflected in a pronounced decrease in probability as seen in fig. 5. Depending on the local geometry steps, small "plateaus" and anisotropic tails may be observed.

In order to compute d_ϕ, auto-correlation functions $C_{II}(R)$ of $\bar{I}$ are considered [52]. If $\bar{I}$ displays exponential decay with a localization length l, C_{II} behaves as $R \exp(-R/l)$ for large R. In fig. 6 auto-correlation functions $C_{II}(R)/R$ of time-averaged probability distributions of the Green's functions corresponding to quantum percolation

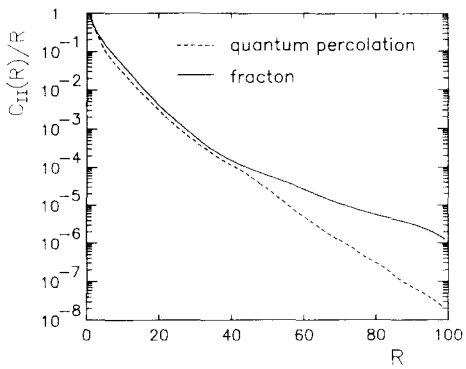

Fig. 6. Auto-correlation functions of time-averaged probability distributions of the Green's function for the quantum percolation model and fracton model. C_{II} is normalized at $R = 0$. Exponential behavior of C_{II} indicates exponential behavior of eigenstates.

(see fig. 4) and fractons are shown. Both curves have been computed from an average of twenty runs. Exponential-like behavior is seen. For the fracton model there is a cross-over at a certain length scale from exponential behavior with a localization length comparable to the quantum percolation case to exponential behavior with a much larger localization length. This cross-over reflects the two "regimes" of localization lengths displayed in fig. 3. The asymptotic spatial behavior is determined by the eigenstates with $l(E) \propto E^{-\bar{d}/2D}$. A best fit for the data for quantum percolation gives $d_\phi = 0.98 \pm 0.04$. For the fracton model one finds $d_\phi = 0.99 \pm 0.05$. For fig. 5 and many other wave packets for both models $d_\phi \simeq 1$ is obtained. These results are not in agreement with the theoretical predictions for d_ϕ. No evidence for the idea of superlocalization on fractal lattices has been obtained.

Using other methods Yakubo et al. [49] have found $d_\phi \simeq 2.3$ for the fracton model. This value was obtained by averaging many eigenstates and does not agree with any of the predicted theoretical values. As discussed above, there are generally two basic structure for the eigenstates: a short-scaled "bulk"-like probability distribution and an asymptotic exponential-like tail. Yakubo et al. did not observe the latter structure. The value $d_\phi \simeq 2.3$ is probably due to averaging the short-scaled structure. A recent analysis [53], employing the same technique as Yakubo et al. [49], has displayed these asymptotic exponential-like tails. Calculations performed on Sierpinski carpets [54] have also displayed exponentially localized behavior. Exponential behavior for the asymptotic spatial decay of eigenstates of the quantum percolation model and fracton model was also inferred by Li et al. [50], using the strip-technique (see section 1.1). With the same technique and using an additional scaling assumption involving d_ϕ, it was inferred [55] recently that superlocalized behavior for fractons does exist with $d_\phi = \zeta_c$. This result is clearly not in agreement with the above-mentioned direct numerical computations [48,53,54] of wave functions. In these studies, wave functions were calculated in real space on lattices large enough to accomodate the localized solutions without invoking any finite-size scaling assumptions.

Some Raman scattering experiments [14] have been interpreted in such a way that indications for superlocalization seem to have been observed. It has been shown [56], however, that the theoretical expressions employed in fact do not contain the exponent d_ϕ at all. Moreover, matrix elements of averaged wave functions on fractal structures may very well not be equal to averaged matrix elements of fractal wave functions [56,57]. It seems that it is not yet clear how to describe properly the scattering of light from fractal structures [57]. Numerical simulations [57] of Raman scattering for the fracton model gave results which are inconsistent with any of the usual theoretical descriptions.

The simple parametrization (1.2), together with eq. (1.1), may not be sufficient to characterize completely excitations and matrix elements of eigenstates on fractals; additional exponent(s) may be required [56]. It has also been pointed out [26,53] that *average* and *typical* wave functions are not necessarily the same.

Summarizing our work, we have demonstrated that eigenstates of two models defined on percolating clusters in two dimensions are localized due to the intrinsic disorder in the geometry. For the fracton model, the energy dependence of localization lengths at the lower band edge was shown to agree with theory. Analysis of the

asymptotic behavior of wave functions gave no evidence for the existence of superlocalization. Two typical characteristics of wavefunction were observed: A bulk-like short-ranged structure and asymptotic exponential tails.

5. Prospects

The use of accurate and efficient product formula algorithms to solve the time-dependent Schrödinger equation has proved to be a useful tool in studying a number of problems. These numerical algorithms can readily be applied to other models in condensed matter physics. At present, we are performing calculations on the two-dimensional $s = \frac{1}{2}$ quantum Heisenberg model.

An interesting new field of research is the study of problems involving disorder and nonlinear interactions. Nonlinearity may strongly influence localization and fluctuation phenomena. Transport and scattering problems in such media could in principle be analyzed with the same methods as in the present work.

Scattering and transport properties of waves in fractal media are interesting subjects. Adequate theoretical descriptions, see previous section, are still lacking. Whether numerical simulations can give new insights is at present unknown *.

Acknowledgements

This work is part of the research program of the Stichting voor Fundamenteel Onderzoek der Materie (FOM), which is financially supported by the Nederlandse Organisatie voor Wetenschappelijk Onderzoek (NWO). We also acknowledge support from the Stichting Nationale Computer Faciliteiten (NCF).

* It was shown very recently that results on bond-percolation networks concerning scattering are easier to interpret [58]. In a recent work the multifractal nature of fractons has been demonstrated. This result implies that smoothing and averaging procedures do not necessarily give unique result due to the intrinsic large amplitude fluctuations [59].

References

[1] P.W. Anderson, Phys. Rev. 109 (1958) 1493.
[2] Y. Nagaoka and H. Fukayama, eds., Anderson localization, (Springer, Berlin, 1982).
B. Kramer, G. Bergmann and Y. Bruynseraede, eds., Localization, Interaction, and Transport Phenomena (Springer, Berlin, 1984).
T. Ando and H. Fukayama, eds., Anderson Localization (Springer, Berlin, 1988).
[3] B. Souillard, in: Chance and Matter, Proc. Les Houches Summer School, Session XLVI, J. Souletie, J. Vannimenus and R. Stora, eds. (Elsevier, Amsterdam, 1987).
[4] F. Delyon, Y. Lévy and B. Souillard, Phys. Rev. Lett. 55 (1985) 618.
[5] A.D. Zdetsis, C.M. Soukoulis, E.N. Economou and G.S. Grest, Phys. Rev. B 32 (1985) 7811.
[6] J.L. Pichard and G. Sarma, J. Phys. C 14 (1981) L127, L617; 18 (1985) 3457.
[7] A. MacKinnon and B. Kramer, Phys. Rev. Lett. 47 (1981) 1546; 49 (1982) 695.
[8] A. MacKinnon and B. Kramer, Z. Phys. B 53 (1983) 1.
[9] E.N. Economou, C.M. Soukoulis, M.H. Cohen and A.D. Zdetsis, Phys. Rev. B 31 (1985) 6172.
[10] H. De Raedt and P. de Vries, Z. Phys. B 77 (1989) 243.
[11] S. John, Comments Condens. Matt. Phys. 14, (1988) 193.
P. Sheng, ed., Classical Wave Localization (World Scientific, Singapore, 1990).
[12] R. Orbach, Science 231 (1986) 814, and references therein.
[13] S. Havlin and D. Ben-Avraham, Adv. Phys. 36 (1987) 695, and references therein.
[14] R. Vacher and E. Stoll, Physica D 38 (1989) 41.
[15] S. Alexander and R. Orbach, J. Phys. (Paris) Lett. 43 (1982) L625.
[16] R. Rammal and G. Toulouse, J. Phys. (Paris) Lett. 44 (1983) L13.
[17] S.J. Lewis and R.B. Stinchcombe, Phys. Rev. Lett. 52 (1984) 1021.
[18] I. Webman and G.S. Grest, J. Phys. (Paris) Lett. 45 (1984) L1155.
[19] S.N. Evangelou, Phys. Rev. B 33 (1986) 3602.
[20] K. Yakubo and T. Nakayama, Phys. Rev. B 36 (1987) 8933.
[21] J.-M. Normand, H.J. Hermann and M. Hajjar, J. Stat. Phys. 52 (1988) 441.
[22] E. Stoll and E. Courtens, Z. Phys. B 81 (1990) 1.
[23] I. Webman and G.S. Grest, Phys. Rev. B 31 (1985) 1689.
[24] A. Aharony, S. Alexander, O. Entin-Wohlman and R. Orbach, Phys. Rev. Lett. 58 (1987) 132.
[25] Y.E. Lévy and B. Souillard, Europhys. Lett. 4 (1987) 233.
[26] A. Brooks Harris and A. Aharony, Europhys. Lett. 4 (1987) 1355.
[27] R. Alben M. Blume, H. Krakauer and L. Schwartz, Phys. Rev. B 12 (1975) 4090.
[28] D.L. Weaire and E.P. O'Reilly, J. Phys. C 18 (1985) 1401.

[29] V.M. Dwyer and D.L. Weaire, Philos. Mag. B 53 (1986) L35.
[30] A. MacKinnon, in: Solid State Science 85, D.G. Pettifor and D.L. Weaire, eds. (Springer, Berlin, 1985).
[31] H.F. Trotter, Proc. Am. Math. Soc. 10 (1959) 545.
[32] M. Suzuki, Prog. Theor. Phys. 56 (1976) 1454.
[33] M. Suzuki, S. Miyashita and A. Kuroda, Prog. Theor. Phys. 58 (1977) 1377.
[34] H. De Raedt and A. Lagendijk, Phys. Rep. C 127 (1985) 233.
[35] H. De Raedt, Comput. Phys. Rep. 7 (1987) 1.
[36] D. Van Dyck, Advances in Electronics and Electron Physics Vol. 65 (Academic, New York, 1985).
[37] M.D. Feit, J.A. Fleck, Jr. and A. Steiger, J. Comput. Phys. 47 (1982) 412.
[38] D. Weaire and A.R. Williams, J. Phys. C 10 (1977) 1239. D. Weaire and V. Srivastava, J. Phys. C 10 (1977) 4309.
[39] M. Suzuki, Phys. Rev. B 31 (1985) 2957.
[40] M. Suzuki, J. Math. Phys. 26 (1985) 601.
[41] B. De Raedt and H. De Raedt, Phys. Rev. A 28 (1983) 3575.
[42] M. Suzuki, Phys. Lett. A 146 (1990) 319.
[43] M. Born and E. Wolf, Principles of Optics (Pergamon, Oxford, 1986).
[44] M.D Feit and J.A. Fleck Jr., Appl. Opt. 18 (1979) 2843.
[45] S. Kirkpatrick and T.P. Eggarter, Phys. Rev. B 6 (1972) 3598.
[46] I.M. Sokolov, Sov. Phys. Usp. 29 (1986) 924, and references therein.
[47] P. de Vries, Ph.D. thesis, University of Amsterdam (1991).
[48] P. de Vries, H. De Raedt and A. Lagendijk, Phys. Rev. Lett. 62 (1989) 2515.
[49] K. Yakubo and T. Nakayama, Phys. Rev. B 40 (1989) 517.
[50] Q. Li, C.M. Soukoulis and G.S. Grest, Phys. Rev. B 41 (1990) 11713.
[51] H.J. Hermann and H.E. Stanley, J. Phys. A 21 (1988) L829.
[52] S. Yoshino and M. Okazaki, J. Phys. Soc. Jpn. 43 (1977) 415.
[53] H. Eduardo Roman, S. Russ and A. Bunde, Phys. Rev. Lett. 66 (C) (1991) 1643.
[54] R. Bourbonnais, R. Maynard and A. Benoît, J. Phys. (Paris) 50 (1989) 3331.
[55] C.J. Lambert and G.D. Hughes, Phys. Rev. Lett. 66 (1991) 1074.
[56] S. Alexander, Phys. Rev. B 40 (1990) 7953.
[57] M. Montagna, O. Pilla, G. Viliani, V. Mazzacurati, G. Ruocco and G. Signorelli, Phys. Rev. Lett. 65 (1990) 1136.
V. Mazzacurati et al., Phys. Rev. B 45 (1992) 2126.
[58] E. Stoll, M. Kolb and E. Courtens, Phys. Rev. Lett. 68 (1992) 2472.
[59] A. Petri and L. Pietronero, Phys. Rev. B 45 (1992) 12864.